Electron Spectroscopy, Molecular Structures, and Binding Energies of Al- and Cu-Imidazole

Xu Wang, Jung Sup Lee, and Dong-Sheng Yang*

Department of Chemistry, University of Kentucky, Lexington, Kentucky 40506-0055

Received: August 2, 2006; In Final Form: September 29, 2006

Al- and Cu-imidazole are produced in laser-vaporization supersonic molecular beams and studied with pulsed field ionization−zero electron kinetic energy (ZEKE) spectroscopy and second-order Møller−Plesset (MP2) theory. The σ and π structures of these complexes are predicted by MP2 calculations, but only the σ structures are identified by the experimental measurements. For these σ structures, adiabatic ionization energies and several vibrational frequencies are measured from the ZEKE spectra, the ground electronic states of the neutral and ionized complexes are determined by comparing the observed and calculated spectra, and the metal−ligand bond dissociation energies of the neutral states are derived by using a thermochemical relation. The measured vibrational modes include the metal−ligand stretch and bend and ligand ring distortions. The metal−ligand stretch frequencies of these transient complexes are compared with those of coordinately saturated, stable metal compounds, and the ligand-based distortion frequencies are compared with those of the free ligand. Al-imidazole has a larger bond dissociation energy than Cu-imidazole, although the opposite order was previously found for the corresponding ions. The weaker bonding of the Cu complex is attributed to the antibonding interaction and the electron repulsion between the Cu 4s and N lone-pair electrons.

I. Introduction

Imidazole, or 1,3-diazole, occurs as an essential constituent in common biological compounds and is one of the most versatile binding sites in proteins. Familiar examples of these biological chemicals include biogenic histamine, amino acid histidine, and the nucleobases adenine and guanine. Derivatives of imidazole are present in antibacterial, antifungal, antiprotozoal, and antihelminthic medications;[1,2] metal ion complexes containing imidazole rings are used as metal corrosion inhibitors[3,4] and potential anticancer agents.[5] Imidazole has a five-membered planar ring structure (Figure 1). In this ring structure, N1 contributes two *p* electrons; N3 and three carbon atoms each provide one *p* electron to form the sextet aromatic π system. Additionally, N3 has a lone pair of electrons in the plane of the molecule. Thus, imidazole is expected to function as an aromatic π ligand or a simple σ ligand in binding with atomic or molecular species.[6]

The widespread applications and multiple binding sites of imidazole have stimulated considerable interest in the binding and structures of its complexes with noble gases, nonpolar and polar molecules, and metal ions. A π-bond structure of a neutral imidazole−Ar complex with Ar on top of the five-membered ring has been determined by rotational millimeter wave spectroscopy in a supersonic jet.[7] The π bonding in imidazole−Ar is, however, changed to the H bonding in (imidazole)$^+$−Ar and $-N_2$, as probed by gas-phase infrared photodissociation spectroscopy and second-order Møller−Plesset (MP2) theoretical calculations.[8] Upon binding with water, N−H···OH_2 and N···H−OH H-bond isomers of imidazole−H_2O have been detected by matrix isolation infrared[9] and Rydberg electron-transfer spectroscopy.[10] For metal complexes, binding energies of a series of metal ions (Li^+, Na^+, K^+, Mg^+, Al^+, Ca^+, Sc^+, Ti^+, V^+, Cr^+, Mn^+, Fe^+, Co^+, Ni^+, Cu^+, and Zn^+) have been measured by collision-induced dissociation,[11−14] and the metal ions in these complexes have been predicted to be σ-bound to the N3 group of imidazole.[11−17] However, there has been no electronic-vibrational spectroscopy reported for any metal−imidazole complexes, and such spectroscopic measurements should provide direct and quantitative evidence about their bonding and structures.

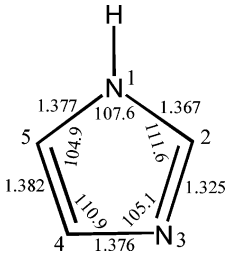

Figure 1. Structure of imidazole from MP2/6-311+G(d,p) calculations. Bond distances are in angstroms, and bond angles are in degrees. This molecule has a permanent electric dipole moment of 3.8 D (ref 38).

Recently, we have developed applications of molecular beam pulsed field ionization−zero electron kinetic energy (ZEKE) spectroscopy to study metal complexes of aromatic hydrocarbons[18,19] and heterocycles.[20] We seek to perform systematic measurements for metal−ligand systems more akin to condensed-phase organometallic and coordination chemistry, by varying the type of the organic ligands attached to metal atoms and the identity of the metals. The major motivation is to explore whether the results of such gas-phase studies show any bonding trends, and how they compare with condensed-phase measurements. In the present study, we examine the Al− and Cu−imidazole complexes using ZEKE spectroscopy and ab initio calculations. Neutral and ionic ground electronic states of these complexes are established by comparing the experiment to theory. Adiabatic ionization energies (AIEs) and metal−ligand

* Corresponding author. E-mail: dyang0@uky.edu.

10.1021/jp0649605 CCC: $33.50
Published on Web 11/09/2006

vibrational frequencies are measured from the ZEKE spectra, and the neutral metal−ligand bond energies are derived using a thermochemical relation.

II. Experimental and Computational Methods

The experimental setup has been described in a previous publication.[21] Al− and Cu−imidazole were prepared by reactions of metal atoms with imidazole vapor in molecular beams. The metal atoms were produced by pulsed laser vaporization of an Al or Cu rod (Al, 99.9999%, Aldrich; Cu, 99.9%, Alfa Aesar) with the second harmonic output of a Nd:YAG laser (Quanta-Ray GCR-3, 532 nm, ∼3 mJ) in the presence of a carrier gas (He or Ar, ultrahigh purity, Scott-Gross) at ∼50 psi. The carrier gas was delivered by a piezoelectric pulsed valve.[22] The metal rod was translated and rotated by a motor-driven mechanism to ensure that each laser pulse ablated a fresh surface. Since imidazole is a solid (mp, 89−91 °C) and has a relatively low vapor pressure at room temperature, a Cu oven was used to obtain sufficient ligand vapor. During the experiment, the oven was heated to about 45 °C by a heating cartridge, and the temperature was maintained by a thermo-controller (Omega CN2110). The vaporized ligand interacted with the metal atoms entrained in the carrier gas.

The Al− and Cu−imidazole complexes in the molecular beams were identified by photoionization time-of-flight mass spectrometry. Ionization was carried out by a frequency-doubled dye laser (Lumonics HD-500), pumped by a XeCl excimer laser (Lumonics PM-884). The production of the 1:1 metal−ligand complexes was maximized by optimizing the timing and power of the vaporization and photoionization lasers, the amount of the ligand vapor, and the backing pressure of the carrier gas. Prior to ZEKE experiments, ionization thresholds of these complexes were measured by recording the ion signals as a function of the laser wavelength. ZEKE electrons were produced by photoexcitation of neutral molecules to high-lying Rydberg states, followed by an ∼3 μs delayed, pulsed electric field ionization (1.2 V cm^{-1}, 100 ns) of these Rydberg states. A small dc field of ∼0.08 V cm^{-1} was applied to help separate the ZEKE from kinetic electrons produced by direct photoionization. The pulsed electric field was generated by a delay pulse generator (Stanford Research System, DG535). The ion and electron signals were detected by a dual microchannel plate detector (Galileo), amplified by a preamplifier (Stanford Research System, SR445), averaged by a gated integrator (Stanford Research System, SR250), and recorded in a laboratory computer. Laser wavelengths were calibrated against vanadium or titanium atomic transitions in regions of the ZEKE spectra.[23] The field dependence of the ZEKE signal was not measured; however, the energy shift from the small electric field (∼1 V cm^{-1}) has been shown to be much smaller than the spectral line width.[19]

Calculations of molecular geometries and vibrational frequencies were carried out by using the MP2/6-311+G(d,p) method, implemented in the Gaussian 03 program.[24] Multidimensional Franck−Condon (FC) factors were computed from the equilibrium geometries, harmonic frequencies, and normal modes of the neutral and ionic complexes.[25,26] The Duschinsky effect[27] was considered to account for the normal mode differences between the neutral molecule and the ion in the FC calculations. Spectral broadening was simulated by giving each line a Lorentzian line shape with the line width of the experimental spectrum. Boltzmann distributions were used to simulate spectra at specific vibrational temperatures.

III. Results and Discussion

A. Ab Initio Calculations. Both σ and π bonding modes are considered in the search for the structures of the Al− and Cu−imidazole complexes and their ions. Metal binding to N3 is considered for the σ structure, and metal binding at the top of the imidazole ring is assumed for the π structure. Figure 2 presents the optimized metal−ligand distances, electronic energies, and ionization and dissociation energies of the σ and π structures. The bond lengths and angles of imidazole in these complexes are similar to those of the free ligand in Figure 1.

1. Al−Imidazole. Since the σ structure of Al−imidazole is expected to be planar, our initial calculations were performed under the C_s point group with Al binding to N3 (Figures 1 and 2). The ground electron configuration of Al is $3s^2 3p^1$; the $3p^1$ electron should be located in one of two $3p_\pi$ orbitals to minimize the repulsion with the N lone-pair electrons. These $3p_\pi$ orbitals are either perpendicular to or in the molecular plane, but are both perpendicular to the Al−N bond. If the $3p^1$ electron is filled in the $3p_\pi$ orbital in the molecular plane, the σ complex will have a $^2A'$ electronic state. On the other hand, if the $3p^1$ electron is filled in the $3p_\pi$ orbital perpendicular to the plane, it will have a $^2A''$ state. In both cases, the Al $3p_\pi^1$ electron will be located in the highest occupied molecular orbital (HOMO), as it has a higher energy than the HOMO of the ligand. Our geometry optimizations show that the $^2A'$ state is 15.7 kJ mol^{-1} lower than the $^2A''$ state. However, subsequent frequency calculations yield an imaginary frequency of 100i cm^{-1} for the $^2A'$ state, and this imaginary frequency still exists in calculations with more stringent convergence criteria. Thus, the $^2A'$ state can be considered a saddle point on the potential energy surface. To search for a minimum energy structure associated with this Al $3p_\pi^1$ electron configuration, we carried out additional calculations without symmetry constrain, that is, under the C_1 point group. The optimization of the C_1 initial geometry yields an essentially planar C_s structure, with dihedral angles (e.g., ∠Al−N3−C2−N1 and ∠Al−N3−C4−C5) smaller than 0.01 degrees, and the resultant electronic state can be described as $^2A'$ under the C_s symmetry. This $^2A'$ state is a minimum (no imaginary frequency); it has a slightly lower electronic energy (2.2 kJ mol^{-1}) than and slightly different bond lengths and angles from the $^2A'$ saddle point obtained by the optimization of the C_s initial geometry.

This $^2A'$ state is 17.9 kJ mol^{-1} more stable and has an Al−N distance 0.089 Å shorter than that of the $^2A''$ state. The geometries of the ligand, however, are quite similar in the two doublet states of the complex and the singlet ground state of free imidazole. Although the interaction between the Al $3p_\pi^1$ and N lone-pair electrons is small and comparable in these doublet states, the Al $3p_\pi^1$ electron of the $^2A'$ state should have a certain degree of repulsion with the $1s^1$ electrons of the adjacent hydrogen atoms, whereas the Al $3p_\pi^1$ electron of the $^2A''$ state should have some repulsion with the π electron cloud of the imidazole ring. The stronger metal−ligand bonding of the $^2A'$ state probably suggests a smaller repulsion between the Al $3p_\pi^1$ and H $1s^1$ electrons than that between the Al $3p_\pi^1$ and the π-electron cloud. Ionization of either the $^2A'$ or $^2A''$ states removes the Al $3p_\pi$-based nonbonding electron from the HOMO and yields the ion ground electronic state of $^1A'$. From the neutral $^2A'$ or $^2A''$ state to the ion $^1A'$ state, the ligand geometry undergoes a small change in bond lengths (< 0.020 Å) and bond angles (< 1.50°), but the Al−N distance is reduced by more than 0.2 Å. The small change in the ligand framework is not surprising, as the ejected electron has an Al-based nonbonding character. The large reduction in the Al−N bond length is due

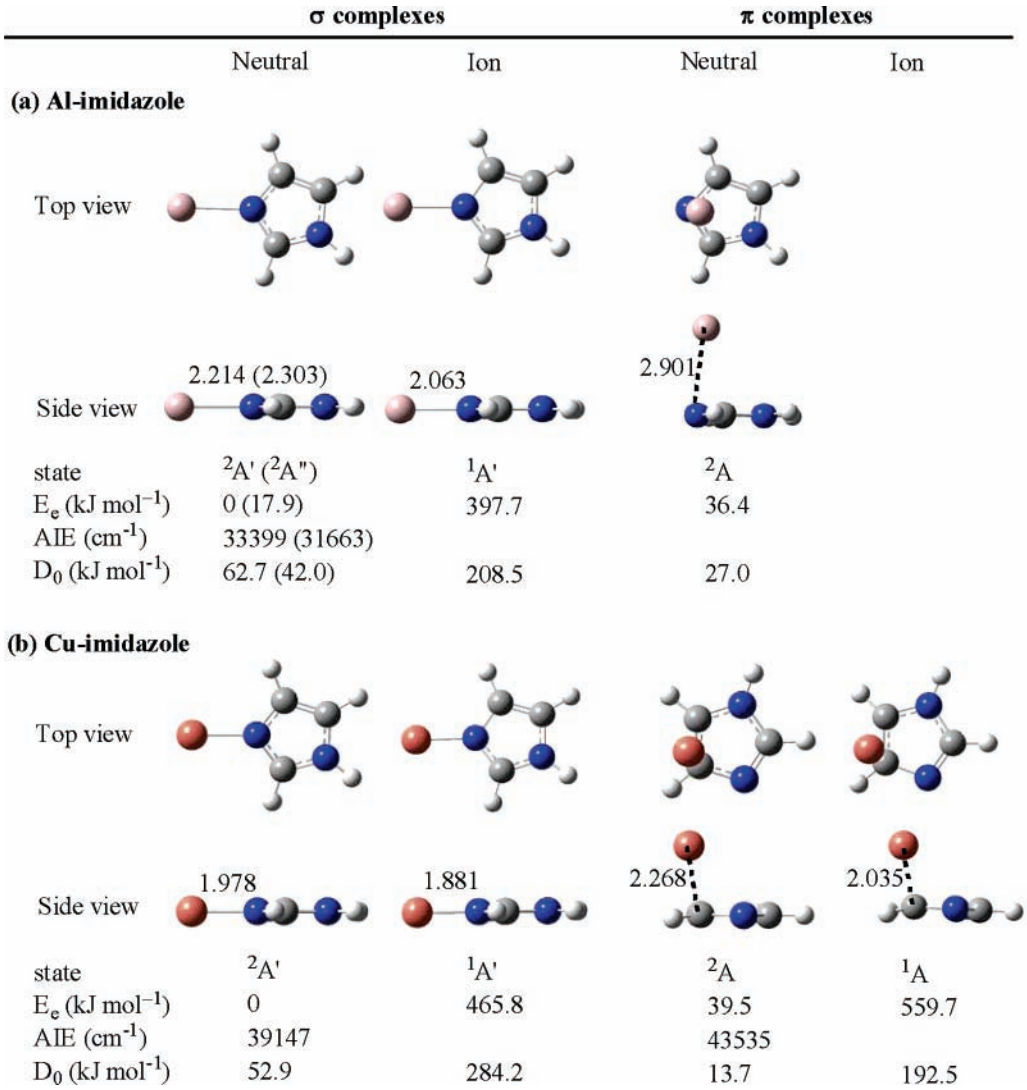

Figure 2. σ and π structure of Al−imidazole (a) and Cu−imidazole (b) from MP2/6-311+G(d,p) calculations. Bond distances are in angstroms. AIE = adiabatic ionization energy; D_0 = metal−ligand bond dissociation energy.

to an additional charge−dipole attraction. Consistent with the reduction of the Al−N bond length is a large increase in the bond dissociation energy from 62.7 (^{2}A′) or 42.0 (^{2}A″) kJ mol^{-1} to 208.5 kJ mol^{-1}.

In addition, our calculations predict a less stable π structure at 36.4 kJ mol^{-1}. In this π structure, Al is located above the five-membered ring and closer to N3 and C4. The Al−N3 and Al−C4 distances are calculated to be 2.901 and 2.990 Å, respectively, whereas the distances between Al and other ring atoms are in the range of 3.240−3.580 Å. The longer metal−ligand distances and smaller dissociation energy (27.0 kJ mol^{-1}) than that of the σ structure are consistent with the common wisdom that imidazole is a weak π ligand. In free imidazole, N3, C4, and C5 atoms carry negative π charges, whereas N1 and C2 bear positive ones.[1] The prediction of the preferred Al binding sites of N3 and C4 indicates that the ligand functions as a weak π donor, in agreement with the viewpoint that imidazole is a weakly π-excessive system.[1] Ionization of the π complex yields the same σ ion structure as the one from ionization of the σ complex. We attempted to search for a stable π ion by starting from the optimized π structure of the neutral molecule and several initial π geometries of the ion, but no π structure was found for the ionized species. The conversion from the neutral π structure to the ionic σ structure shows that predominant binding in the ionized species is the charge−dipole attraction.

2. Cu−Imidazole. The σ structure of the neutral Cu−imidazole has C_s symmetry and a ^{2}A′ ground electronic state (Figure 2). The HOMO of the ^{2}A′ ground state is formed by an antiphase σ^* interaction between the Cu 4s^1 and N lone-pair electrons. The electron repulsion is strong since both the Cu 4s and N lone-pair orbitals are along the Cu−N axis. Because of the spherical shape of the s orbital, this complex has no ^{2}A″ electronic state. Ionization of the ^{2}A′ neutral ground-state yields a ^{1}A′ ion ground state in C_s symmetry. From the ^{2}A′ to ^{1}A′ state, the copper−nitrogen distance is reduced from 1.978 Å to 1.881 Å, and the metal−ligand dissociation energy is increased from 52.9 to 284.2 kJ mol^{-1}. These bonding and structural changes are due to the removal of the antibonding σ^* electron in the ^{2}A′ neutral state and the addition of a charge−dipole interaction in the ^{1}A′ ion state. Compared to the Al−imidazole σ complex, the neutral bond energy is smaller, but the ionic bond energy is larger. These differences between the Cu and Al complexes will be discussed in Section IIIC.

The neutral ^{2}A ground electronic state of the π structure is located 39.5 kJ mol^{-1} above the ^{2}A′ state of the σ structure. In this π structure, the Cu atom is nearly on top of the C4−C5

TABLE 1: Observed Transitions and Assignments for the ZEKE Spectra of Al− and Cu−Imidazole σ Complexes

Al−imidazole				Cu−imidazole			
$^1A' \leftarrow {}^2A'$				$^1A' \leftarrow {}^2A'$			
positions	assignments	positions	assignments	positions	assignments	positions	assignments
35 119	16_1^0	36 386	$16_0^3\,17_0^1$	42 054	0_0^0	42 747	$16_0^2\,17_1^1\,24_1^1$
35 343	0_0^0	36 408	13_0^1	42 088	24_1^1	42 754	$16_0^2\,17_2^2$
35 378	24_1^1	36 535	11_0^1	42 103	17_1^1	42 796	$16_0^2\,17_2^2\,24_1^1$
35 413	24_2^2	36 555	16_0^4	42 137	$17_1^1\,24_1^1$	42836	$16_0^2\,17_0^1$
35 470	17_0^1	36 599	$16_0^4\,24_1^1$	42 227	17_0^1	42 922	$16_0^2\,24_1^3$
35 506	$17_0^1\,24_1^1$	36 629	$16_0^4\,24_2^2$	42 359	16_0^1	42 965	16_0^3
35 653	16_0^1	36 682	$16_0^4\,17_0^1$	42 397	$16_0^1\,24_1^1$	43 001	$16_0^3\,24_1^1$
35 689	$16_0^1\,24_1^1$	36 717	$13_0^1\,16_0^1$	42 410	$16_0^1\,17_1^1$	43 015	$16_0^3\,17_1^1$
35 730	$16_0^1\,24_2^2$	36 758	$13_0^1\,16_0^1 24_1^1$	42 436	$16_0^1\,24_2^2$	43 053	$16_0^3\,17_1^1 24_1^1$
35 781	$16_0^1\,17_0^1$	36 843	$11_0^1\,16_0^1$	42 450	$16_0^1\,17_1^1 24_1^1$	43 104	$16_0^3\,17_2^2 24_1^1$
35 817	$16_0^1\,17_0^1 24_1^1$	36 848	16_0^5	42 459	$16_0^1\,17_2^2$	43 132	$16_0^3\,17_0^1$
35 956	16_0^2	37 022	$13_0^1\,16_0^2$	42 485	$16_0^1\,17_1^1 24_2^2$	43 183	13_0^1
35 995	$16_0^2\,24_1^1$	37 060	$13_0^1\,16_0^2 24_1^1$	42 532	$16_0^1 17_0^1$	43 238	$16_0^3\,24_1^3$
36 033	$16_0^2\,24_2^2$			42 580	$16_0^1\,24_0^2$	43 269	16_0^4
36 085	$16_0^2\,17_0^1$			42615	$16_0^1\,24_1^3$	43325	$16_0^4\,17_1^1$
36 258	16_0^3			42 662	16_0^2	43 438	$16_0^4\,17_0^1$
36 296	$16_0^3\,24_1^1$			42 703	$16_0^2\,24_1^1$	43 489	$13_0^1\,16_0^1$
36 332	$16_0^3\,24_2^2$			42 710	$16_0^2\,17_1^1$	43 573	16_0^5

bond, and the Cu−C4 and Cu−C5 distances are calculated to be 2.269 and 2.328 Å, respectively. The distances between Cu and other ring atoms are much longer and in the 2.940−3.240 Å range. The stronger Cu binding to C4 and C5 atoms (compared to other ring atoms) is also evident from a larger increase in the C4−C5 bond length (from 1.382 Å in the free ligand to 1.399 Å in the π complex). Like Al−imidazole, the metal-ring distances are longer, and the bond energy is smaller than that of the σ structure. A significant difference from Al−imidazole is that the π structure of Cu−imidazole remains intact upon ionization. In this π ion, the Cu atom moves close to C4 and C5, with the Cu−C4 and −C5 distances being reduced to 2.035 and 2.254 Å, respectively, and the C4−C5 bond length being increased to 1.422 Å. These structural changes are in line with the increase in the metal−ligand dissociation energy in the ion.

B. ZEKE Spectra. Figures 3−6 present the experimental and theoretical ZEKE spectra, and Table 1 lists the energies of observed transitions and their assignments. The spectral assignments are discussed by comparing them with similar molecular species and with spectral simulations. In these simulations, the theoretical vibrational frequencies are not scaled, while the calculated 0−0 transition energies are shifted to the measured values for simplicity.

1. Al−Imidazole. Figure 3a shows the ZEKE spectrum of Al−imidazole seeded in He carrier gas. The first strong peak at 35343 (5) cm^{-1} has a line width of 10 cm^{-1} and is assigned to the 0−0 transition between the ground vibronic levels of the neutral and ionic complexes. Above the 0−0 transition, the spectrum shows a main progression (16_0^n) of 310 cm^{-1} spacing with up to five vibrational quanta and three other progressions formed by combinations of the 310 cm^{-1} spacing with 127 ($16_0^n\,17_0^1$), 1065 ($13_0^1\,16_0^n$), or 1192 cm^{-1} ($11_0^1\,16_0^n$) intervals. Additionally, sequence transitions are observed at the higher wavenumber side of these progressions and are measured ~35 or 2× ~35 cm^{-1} from the respective cold transitions. These sequence transitions are labeled $16_0^n\,24_m^m$, $16_0^n\,17_0^1\,24_1^1$, and $13_0^1\,16_0^n 24_1^1$ in the figure. Below the 0−0 transition, a very small peak appears at 224 cm^{-1} (16_1^0) from an excited vibrational level of the neutral electronic ground state to the ground vibrational level of the ionic state. All of these hot transitions disappear in the spectrum recorded with Ar carrier (Figure 4a), because vibrational temperatures of molecules seeded in Ar are lower.[28] Associated with the vibrational cooling, the molecules seeded in Ar also have lower rotational temperatures, as evident from the reduction of the spectral line width from 10 to 7 cm^{-1}.

Previously, vibrational spectra of imidazole have been measured by argon matrix-isolation[9,29] and vapor-phase[30] infrared spectroscopy and by solid-state inelastic neutron scattering.[31] From these measurements and associated ab initio calculations,[9,31] all vibrational modes of this organic compound are larger than 500 cm^{-1}, four of which are in the range of 1050−1200 cm^{-1}. Therefore, the 1065 and 1192 cm^{-1} intervals in the ZEKE spectra should arise from ligand-based vibrations,

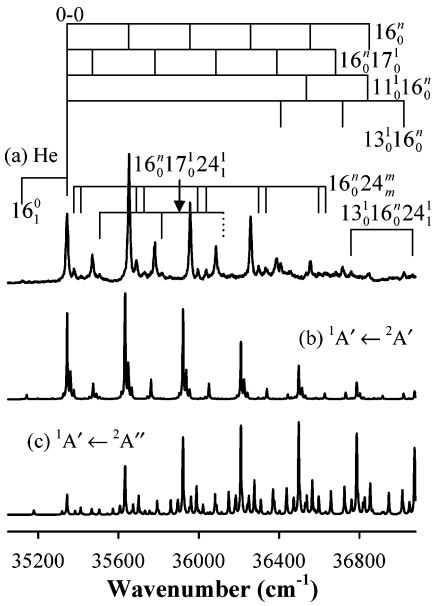

Figure 3. ZEKE spectrum of Al−imidazole seeded in helium (a) and simulations of the $^1A' \leftarrow {}^2A'$ (b) and $^1A' \leftarrow {}^2A''$ (c) transitions of the σ structure at 80 K.

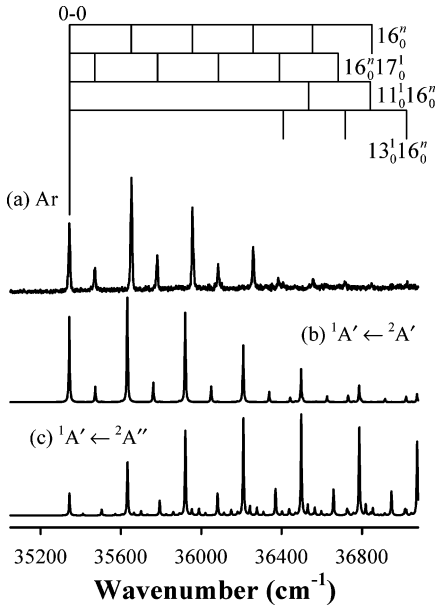

Figure 4. ZEKE spectrum of Al−imidazole seeded in argon (a) and simulations of the $^1A' \leftarrow {}^2A'$ (b) and $^1A' \leftarrow {}^2A''$ (c) transitions of the σ structure at 10 K.

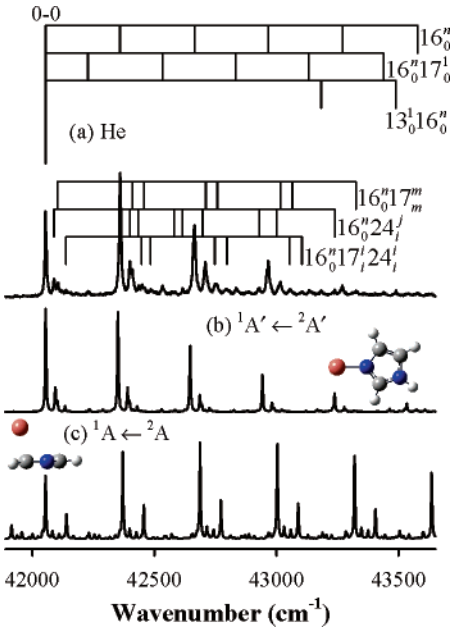

Figure 5. ZEKE spectrum of Cu−imidazole seeded in helium (a) and simulations of the $^1A' \leftarrow {}^2A'$ transition of the σ structure (b) and the $^2A \leftarrow {}^1A$ transition of the π structure (c) at 80 K.

and the 127 and 309 cm^{-1} intervals should arise from metal−ligand vibrations. Furthermore, previous ZEKE measurements[32−34] have found that the Al^+−N stretch frequencies of Al−amine complexes are around 300 ± 60 cm^{-1}. This frequency range suggests that the 308 cm^{-1} spacing may correspond to the Al^+−N stretch as well.

Our MP2 calculations predict the $^2A'$ and $^2A''$ electronic states for the σ structure and the ^2A ground state for the π structure of the neutral complex as well as the $^1A'$ ground state of the ionic complex. Since the three neutral states, especially the two neutral states of the σ structure, are predicted to be close in energy, transitions from these neutral states to the $^1A'$ ion state may be all possible. However, because of their large structural changes, the electronic transition from the ^2A state of the neutral π complex to the $^1A'$ state of the σ ion is expected to have a much longer FC profile than what is observed in the experiment. This transition can thus be excluded from the spectral assignment.

Figures 3b,c and 4b,c show the spectral simulations of the $^1A' \leftarrow {}^2A'$ and $^1A' \leftarrow {}^2A''$ transitions of the σ complex, in comparison with the experimental spectra (Figures 3a and 4a). The $^1A' \leftarrow {}^2A''$ simulations have a significantly longer FC profile and many more transitions than the observed spectra, whereas the $^1A' \leftarrow {}^2A'$ simulations have a very good match with the measured ones. The longer FC profile in the $^1A' \leftarrow {}^2A''$ simulation is due to a larger Al−N distance change from the initial neutral state to the final ion state. On the basis of the agreement between the $^1A' \leftarrow {}^2A'$ simulations and the experimental spectra, we have assigned each of the observed peaks to specific vibronic transitions (Table 1). The 310 cm^{-1} major progression is assigned to the transitions from the ground vibrational level of the neutral $^2A'$ state to the Al^+−imidazole symmetric stretch levels of the ionic $^1A'$ state, ν_{16}^+. A least-squares fit of the peak positions of 16_0^n to $G(v) = \omega_S{}^+ (v^+ + 1/2) + x_{SS}{}^+ (v^+ + 1/2)^2$ yields a harmonic frequency of 312.6 (8) cm^{-1} and an anharmonicity of −1.9 (1) cm^{-1} for this ion stretch mode. The 127 cm^{-1} interval is attributed to an in-plane Al^+−imidazole symmetric bend, ν_{17}^+; the 1065 and 1192 cm^{-1} are ascribed to in-plane imidazole ring distortions, ν_{13}^+ and ν_{11}^+. ν_{13}^+ is largely characterized by an in-plane C−H bend, whereas ν_{11}^+ is described by a C−N stretch. The ν_{13} frequency of the free ligand has been measured to be 1074 cm^{-1} in the vapor phase,[30] 1076 or 1074 cm^{-1} in the argon matrix,[9,29] and 1061 cm^{-1} in the solid.[31] Cu coordination seems to have a small effect on this in-plane C−H bending vibration. The ν_{11} frequency of imidazole has not been reported in the vapor phase, but has been measured as 1124 or 1130 cm^{-1} in the argon matrix[9,29] and 1142 cm^{-1} in the solid state.[31] These frequencies are significantly smaller than that in Al^+−imidazole. However, this difference may not be used to assess the effect of Al coordination to the C−N stretching vibration, as the matrix interaction and H-bonding affect its frequency as well. Although the assignment of the sequence transitions above the band origin does not yield any additional fundamental frequency, a difference between the Al−imidazole out-of-plane bends in the ionized and neutral complexes is determined to be 35 cm^{-1}. The 224 cm^{-1} peak below the band origin is assigned to the Al−imidazole stretch excitation in the neutral complex, ν_{16}.

2. Cu−Imidazole. Figures 5a and 6a present the spectra of Cu−imidazole seeded in He and Ar carriers, respectively. The 0−0 transition energy is measured to be 42054 (5) cm^{-1}, which is higher than that of Al−imidazole [35344 (5) cm^{-1}]. The higher transition energy is in line with the higher ionization energy of Cu atom. The spectral line widths are measured to be 7 cm^{-1} in He and 5 cm^{-1} in Ar. These line widths are significantly narrower than that of Al−imidazole. This is consistent with smaller rotational constants of Cu−imidazole, which may lead to a lower rotational temperature and a less spread rotational envelop. Both Figures 5a and 6a show a major progression of the 305 cm^{-1} spacing and its combinations with 173 ($16_0^n\,17_0^1$) and 1129 cm^{-1} ($13_0^1\,16_0^1$) intervals. In addition to these cold transitions, Figure 5a displays a number of progressions formed by sequence transitions, which are labeled $16_0^n\,17_m^m$, $16_0^n\,24_i^j$, and $16_0^n\,17_m^m\,24_i^i$. These peaks vanish in Figure 6a because of the lower vibrational temperatures of the complex in the heavier gas.

Compared to Al−imidazole, the 305 cm^{-1} progression can be assigned to the Cu^+−imidazole symmetric stretch (ν_{16}^+), the 173 cm^{-1} interval can be assigned to a Cu^+−imidazole in-plane

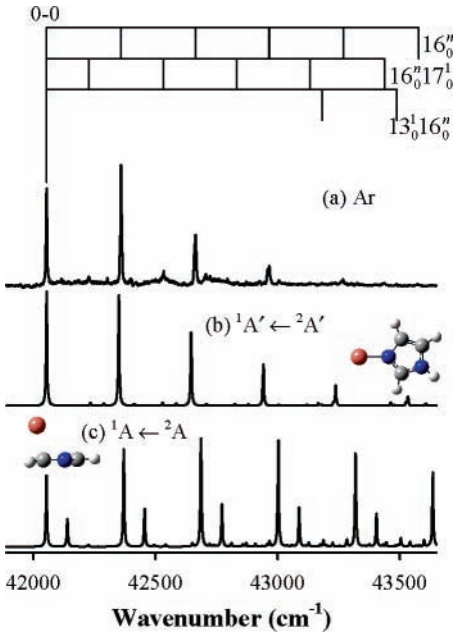

Figure 6. ZEKE spectrum of Cu−imidazole seeded in argon (a) and simulations of the $^1A' \leftarrow {}^2A'$ transition of the σ structure (b) and the $^2A \leftarrow {}^1A$ transition of the π structure (c) at 10 K.

bend (ν_{17}^+), and 1129 cm^{-1} can be assigned to an imidazole ring distortion. Since the 1129 cm^{-1} interval is in the middle of the two ring-distortion frequencies [1065 (ν_{13}^+) and 1192 (ν_{11}^+) cm^{-1}] observed for Al^+−imidazole, this simple comparison cannot decide whether the 1129 cm^{-1} interval is associated with ν_{13}^+ or ν_{11}^+.

To assign the spectra in more details, Figures 5 and 6 compare the experimental spectra with the simulations of the σ and π structures at 80 and 10 K. For the simulations of the π structure, although the frequency interval of the major progression (316 cm^{-1}) is comparable to the experimental value (305 cm^{-1}), the calculated FC intensity is significantly larger. Moreover, an additional cold progression with the spacing of 86 cm^{-1} is predicted, but not observed in the experimental spectra. In contrast, the simulations of the σ structure have very good agreement with the experimental spectra in both the FC intensity and the vibrational frequencies. In addition, the AIE of the σ structure is predicted to be closer to the experimental value. Our previous studies have shown that the MP2 calculations typically underestimate AIE values of Cu−ligand complexes by about 3000 cm^{-1}.[20,35,36] By correcting the 3000 cm^{-1} error, the AIE is estimated to be 42 147 cm^{-1} for the σ structure and 46 535 cm^{-1} for the π structure. Thus, the corrected theoretical AIE of the σ structure has a much better match with the measured value of 42 054 cm^{-1}. Therefore, the comparisons of the FC intensity, vibrational frequencies, and AIE value show that the observed spectra must arise from ionization of the $^2A'$ state of the σ structure, rather than the ^2A state of the π structure.

The good agreement between the experimental spectra and the $^1A' \leftarrow {}^2A'$ simulations of the σ structure confirms the above empirical assignments of the 305 cm^{-1} interval to the Cu^+−imidazole stretch (ν_{16}^+) and the 173 cm^{-1} spacing to the Cu^+−imidazole in-plane bend (ν_{17}^+) in the $^1A'$ ion state. It is also clear that the 1129 cm^{-1} interval is due to the excitation of the ν_{13}^+ ring distortion characterized by an in-plane C−H bend. The assignment of the hot transitions yields the Cu−imidazole in-plane bending frequency of 124 cm^{-1} (ν_{17}) in the $^2A'$ neutral state and the Cu−imidazole out-of-plane bending (ν_{24}) frequencies of 111 and 74 cm^{-1} in the $^1A'$ and ^2A states, respectively.

TABLE 2: AIEs (cm^{-1}), Metal−Ligand Bond Dissociation Energies (D_0 and D_0^+, kJ mol^{-1}), and Vibrational Frequencies (cm^{-1}) of Al− and Cu−Imidazole σ Complexes from the ZEKE Spectra and MP2/6-311+G(d,p) Calculations[a]

		experiment[b]	MP2
Al−imidazole			
AIE		35 343	33 399
D_0^+/D_0		232.4/77.7	208.5/62.7
ring distortion	ν_{11}^+, a′	1192	1164
ring distortion	ν_{13}^+, a′	1065	1100
Al−imidazole symmetric stretch	ν_{16}^+/ν_{16}, a′	313[c]/224	289/202
Al−imidazole in-plane bend	ν_{17}^+, a′	127	129
Al−imidazole out-of-plane bend	ν_{24}^+/ν_{24}, a″	$\nu_{24}^+ - \nu_{24} = 35$	$\nu_{24}^+ - \nu_{24} = 16$
Cu−imidazole			
AIE		42 054	39 147
D_0^+/D_0		287.5/45.1	284.2/52.9
ring distortion	ν_{13}^+, a′	1129	1112
Cu−imidazole symmetric stretch	ν_{16}^+, a′	303[c]	296
Cu−imidazole in-plane bend	ν_{17}^+/ν_{17}, a′	173/124	179/131
Cu−imidazole out-of-plane bend	ν_{24}^+/ν_{24}, a″	111/74	117/78

[a] D_0 and D_0^+ are metal−ligand bond dissociation energies of the neutral and ionic complexes, respectively. [b] The uncertainty of the AIE values is ~5 cm^{-1}. D_0^+ values are taken from ref 13 with an uncertainty of 8.2 kJ mol^{-1} in Al^+−imidazole and 7.4 kJ mol^{-1} in Cu^+−imidazole. D_0 values are obtained by using a thermochemical relation. [c] Harmonic frequencies from least-squares fits.

A least-squares fit of the peak positions of 16_0^n yields a harmonic ν_{16}^+ frequency of 303 (1) cm^{-1} and an anharmonicity of −0.2 (2) cm^{-1}. Interestingly, the stretch frequency of the isolated Cu^+−imidazole complex is almost identical to that of $[Cu^{2+}-(imidazole)_2]Cl_2$ (306.5 cm^{-1}) and $[Cu^+-(imidazole)_2]$-Br_2 (307.0 cm^{-1}) measured in the condensed phase.[37] A similar observation has also been reported for Cu^+−diazine complexes.[20] These observations suggest that the concept of formal oxidation states widely used in inorganic and organometallic chemistry may not reflect true electric charges on coordinated metal positive ions. In addition to anion ligands, the number and type of coordinated neutral ligands affect the amount of the charges on the metal ion.

C. Metal−Ligand Binding in Al− and Cu−Imidazole. Table 2 summarizes the measured ionization and metal−ligand bond dissociation energies and vibrational frequencies of the two complexes. The dissociation energies of the ions were determined by Rodgers and co-workers with collision-induced dissociation,[13] and that of the neutral complexes were derived from a thermochemical cycle by involving the ion dissociation energies and AIEs of the complexes and metal atoms.[38] These measured values are compared with those predicted from the MP2 calculations. The theory predicts the correct order of the ionization and dissociation energies, but underestimates their values. The calculated vibrational frequencies are generally in good agreement with the experimental measurements, although the computational accuracy remains to be improved.

For both complexes, ionization enhances the binding between the metal and ligand, and the stronger ion binding leads to an AIE reduction from the metal atom to the complex. This AIE shift is measured to be 12935 cm^{-1} for Al and 20263 cm^{-1} for Cu. The bond dissociation energy of Al^+−imidazole is smaller than that of Cu^+−imidazole, but the opposite order is observed for the neutral complexes. The stronger Cu^+ ion bonding is easy to understand because Cu^+ is smaller and thus has a stronger

charge−dipole interaction with the ligand. The valence shell radius of Cu^+ (3d) is calculated to be 0.33 Å, whereas the radius of Al^+(3s) is 1.11 Å.[39] In addition to the ion size effect, orbital interactions or electron repulsions also contribute to the binding difference between the two metals. The HOMO of the $^2A'$ neutral state of Al−imidazole is largely the Al $3p_\pi$ character, whereas that of the $^2A'$ neutral state of Cu−imidazole is formed by the antiphase σ^* interaction between the Cu 4s and N lone-pair orbitals. Removal of the σ^* electron by ionization should substantially increase the metal−ligand binding, whereas removal of the mainly nonbonding Al $3p_\pi$ electron should have a small effect. The σ^* interaction also explains why the large bond energy of the Cu^+ ion complex is not carried over into the neutral species, even though the Cu−N bond is shorter than the Al−N bond (Figure 2). The charge−dipole and orbital interactions can also be used to rationalize metal−ligand binding in complexes containing the same metal atoms but different ligands. For example, the bond dissociation energy of Cu^+−imidazole (287.5 kJ mol^{-1}) is larger than that of Cu^+−pyrimidine (249.6 kJ mol^{-1}),[40] because imidazole has a larger electric dipole (3.8 D) and stronger basicity (8.0 pK_b) than pyrimidine (2.334 D, 3.4 pK_b).[38,41,42] On the other hand, the bond energies of the neutral Cu−imidazole (45.1 kJ mol^{-1}) and −pyrimidine (46.4 kJ mol^{-1})[20] are comparable, since the σ^* interactions or electron repulsions are similar in both cases.

The major vibrational progression observed in the ZEKE spectra of the two complexes is from excitation of the cation−ligand symmetric stretch (ν_{16}^+). This spectroscopic observation is consistent with the MP2 prediction, which shows that the largest structural change upon ionization occurs at the metal−nitrogen bond. The harmonic frequency of this stretch mode is measured to be 313 cm^{-1} in Al^+−imidazole and 303 cm^{-1} in Cu^+−imidazole. If one assumes that the metal−ligand stretch in these complexes behaves as diatomic molecules, then the force constant ($k = 4\pi^2c^2\omega^2\mu$, where k is the force constant, c is the speed of light, ω is the harmonic frequency, and μ is the reduced mass) of the Al^+−imidazole stretch is estimated to be about 63% of that of the Cu^+−imidazole stretch. The ratio of the metal−ligand bond energies of these two complexes is about 81%.

IV. Conclusions

We have reported a joint ZEKE spectroscopic and MP2 computational study of Al− and Cu−imidazole. ZEKE spectroscopy measures the AIEs and several vibrational frequencies, and the MP2 calculations predict the σ and π structures, with the former being more stable. By comparing these measurements and calculations, we have determined that the observed spectra arise from ionization of the σ structure. The ground electronic states of the σ Al/Cu− and Al^+/Cu^+−imidazole complexes are $^2A'$ and $^1A'$ in C_s symmetry, respectively. The adiabatic ionization and bond dissociation energies are 35 343 (5) cm^{-1} and 78 (8) kJ mol^{-1} for the $^2A'$ state of the σ Al complex, and 42 054 (5) cm^{-1} and 45 (7) kJ mol^{-1} for the $^2A'$ state of the σ Cu complex. The weaker Cu bonding is due to a stronger electron repulsion and σ^* interaction between the Cu 4s and N lone-pair electrons. The major vibrational progression observed is the metal−ligand stretch, which has frequencies of 313/224 cm^{-1} in Al^+/Al−imidazole and 303 cm^{-1} in Cu^+−imidazole. The stretch frequency in the coordinately unsaturated Cu^+−imidazole complex is nearly identical to those in the stable $[Cu^{2+}-(imidazole)_2]X_2$ (X = Cl, Br) compounds.[37]

Acknowledgment. This work was supported by the Physical Chemistry Program of the National Science Foundation and the donors of the Petroleum Research Fund of the American Chemical Society.

Supporting Information Available: Tables of the geometries and vibrational frequencies of the Al− and Cu−imidazole σ and π complexes from MP2/6-311+G(d,p) calculations. This material is available free of charge via the Internet at http://pubs.acs.org.

References and Notes

(1) Katritzky, A. R.; Pozharskii, A. F. *Handbook of Heterocyclic Chemistry*, 2nd ed.; Pergamon: Amsterdam, 2000.
(2) De Luca, L. *Curr. Med. Chem.* **2006**, *13*, 1.
(3) Lee, W.-J. *Mater. Sci. Eng., A* **2003**, *348*, 217.
(4) Otmacic, H.; Stupnisek-Lisac, E. *Electrochim. Acta* **2003**, *48*, 985.
(5) Zhao, G.; Lin, H. *Curr. Med. Chem.: Anti-Cancer Agents* **2005**, *5*, 137.
(6) Sundberg, R. J.; Martin, R. B. *Chem. Rev.* **1974**, *74*, 471.
(7) Caminati, W.; Melandri, S.; Millemaggi, A.; Favero, P. G. *Chem. Phys. Lett.* **1998**, *294*, 377.
(8) Andrei, B.-S.; Solca, N.; Dopfer, O. *J. Phys. Chem. A* **2005**, *109*, 3598.
(9) Van Bael, M. K.; Smets, J.; Schoone, K.; Houben, L.; McCarthy, W.; Adamowicz, L.; Nowak, M. J.; Maes, G. *J. Phys. Chem. A* **1997**, *101*, 2397.
(10) Carles, S.; Lecomte, F.; Schermann, J. P.; Desfrancois, C. *J. Phys. Chem. A* **2000**, *104*, 10662.
(11) Rodgers, M. T.; Armentrout, P. B. *Int. J. Mass Spectrom.* **1999**, *185/186/187*, 359.
(12) Huang, H.; Rodgers, M. T. *J. Phys. Chem. A* **2002**, *106*, 4277.
(13) Rannulu, N. S.; Amunugama, R.; Yang, Z.; Rodgers, M. T. *J. Phys. Chem. A* **2004**, *108*, 6385.
(14) Rannulu, N. S.; Rodgers, M. T. *Phys. Chem. Chem. Phys.* **2005**, *7*, 1014.
(15) Sletten, E.; Stogard, A. *THEOCHEM* **1987**, *38*, 289.
(16) Alcami, M.; Mo, O.; Yanez, M. *J. Phys. Chem.* **1989**, *93*, 3929.
(17) Alcami, M.; Mo, O.; Yanez, M. *J. Phys. Chem.* **1992**, *96*, 3022.
(18) Sohnlein, B. R.; Li, S.; Yang, D.-S. *J. Chem. Phys.* **2005**, *123*, 214306.
(19) Sohnlein Bradford, R.; Yang, D.-S. *J. Chem. Phys.* **2006**, *124*, 134305.
(20) Wang, X.; Lee, J. S.; Yang, D.-S. *J. Chem. Phys.* **2006**, *125*, 014309.
(21) Rothschopf, G. K.; Perkins, J. S.; Li, S.; Yang, D.-S. *J. Phys. Chem. A* **2000**, *104*, 8178.
(22) Proch, D.; Trickl, T. *Rev. Sci. Instrum.* **1989**, *60*, 713.
(23) Moore, C. E. *Atomic Energy Levels*; National Bureau of Standards: Washington, DC, 1971.
(24) Frisch, M. J.; Trucks, G. W.; Schlegel, H. B.; Scuseria, G. E.; Robb, M. A.; Cheeseman, J. R.; Montgomery, J. A., Jr.; Vreven, T.; Kudin, K. N.; Burant, J. C.; Millam, J. M.; Iyengar, S. S.; Tomasi, J.; Barone, V.; Mennucci, B.; Cossi, M.; Scalmani, G.; Rega, N.; Petersson, G. A.; Nakatsuji, H.; Hada, M.; Ehara, M.; Toyota, K.; Fukuda, R.; Hasegawa, J.; Ishida, M.; Nakajima, T.; Honda, Y.; Kitao, O.; Nakai, H.; Klene, M.; Li, X.; Knox, J. E.; Hratchian, H. P.; Cross, J. B.; Bakken, V.; Adamo, C.; Jaramillo, J.; Gomperts, R.; Stratmann, R. E.; Yazyev, O.; Austin, A. J.; Cammi, R.; Pomelli, C.; Ochterski, J. W.; Ayala, P. Y.; Morokuma, K.; Voth, G. A.; Salvador, P.; Dannenberg, J. J.; Zakrzewski, V. G.; Dapprich, S.; Daniels, A. D.; Strain, M. C.; Farkas, O.; Malick, D. K.; Rabuck, A. D.; Raghavachari, K.; Foresman, J. B.; Ortiz, J. V.; Cui, Q.; Baboul, A. G.; Clifford, S.; Cioslowski, J.; Stefanov, B. B.; Liu, G.; Liashenko, A.; Piskorz, P.; Komaromi, I.; Martin, R. L.; Fox, D. J.; Keith, T.; Al-Laham, M. A.; Peng, C. Y.; Nanayakkara, A.; Challacombe, M.; Gill, P. M. W.; Johnson, B.; Chen, W.; Wong, M. W.; Gonzalez, C.; Pople, J. A. *Gaussian 03*, revision C.02; Gaussian, Inc.: Wallingford, CT, 2004.
(25) Yang, D.-S.; Zgierski, M. Z.; Rayner, D. M.; Hackett, P. A.; Martinez, A.; Salahub, D. R.; Roy, P.-N.; Carrington, T., Jr. *J. Chem. Phys.* **1995**, *103*, 5335.
(26) Berces, A.; Zgierski, M. Z.; Yang, D.-S. *Computational Molecular Spectroscopy*; Wiley: New York, 2000.
(27) Duschinsky, F. *Acta Physicochim. URSS* **1937**, *7*, 551.
(28) Fuller, J. F.; Li, S.; Sohnlein, B. R.; Rothschopf, G. K.; Yang, D.-S. *Chem. Phys. Lett.* **2002**, *366*, 141.
(29) King, S. T. *J. Phys. Chem.* **1970**, *74*, 2133.
(30) Perchard, C.; Bellocq, A.; Novak, A. *J. Chim. Phys.* **1965**, *62*, 1344.
(31) Loeffen, P. W.; Pettifer, R. F.; Fillaux, F.; Kearley, G. J. *J. Chem. Phys.* **1995**, *103*, 8444.
(32) Yang, D.-S.; Miyawaki, J. *Chem. Phys. Lett.* **1999**, *313*, 514.

(33) Li, S.; Rothschopf, G. K.; Fuller, J. F.; Yang, D.-S. *J. Chem. Phys.* **2003**, *118*, 8636.

(34) Li, S.; Fuller, J. F.; Wang, X.; Sohnlein, B. R.; Bhowmik, P.; Yang, D.-S. *J. Chem. Phys.* **2004**, *121*, 7692.

(35) Li, S.; Sohnlein, B. R.; Rothschopf, G. K.; Fuller, J. F.; Yang, D.-S. *J. Chem. Phys.* **2003**, *119*, 5406.

(36) Miyawaki, J.; Sugawara, K.; Li, S.; Yang, D.-S. *J. Phys. Chem. A* **2005**, *109*, 6697.

(37) Cornilsen, B. C.; Nakamoto, K. *J. Inorg. Nucl. Chem.* **1974**, *36*, 2467.

(38) Lide, D. R.; Frederikse, H. P. R. *CRC Handbook of Chemistry and Physics*, 78th ed.; CRC: New York, 1997.

(39) WebElements Home Page. http://www.webelements.com/ (accessed July 2006).

(40) Amunugama, R.; Rodgers, M. T. *J. Phys. Chem. A* **2001**, *105*, 9883.

(41) Houriet, R.; Schwarz, H.; Zummack, W.; Andrade, J. G.; Schleyer, P. V. R. *Nouv. J. Chim.* **1981**, *5*, 505.

(42) Taft, R. W.; Anvia, F.; Taagepera, M.; Catalan, J.; Elguero, J. *J. Am. Chem. Soc.* **1986**, *108*, 3237.